Fluorescence Properties of Hydrophilic Semiconductor Nanoparticles with Tridentate Polyethylene Oxide Ligands

Marc Thiry,[†,§] Klaus Boldt,[†,§] Marija S. Nikolic,[‡] Florian Schulz,[†] Michael Ijeh,[†] Andjana Panicker,[†] Tobias Vossmeyer,[†] and Horst Weller[†,*]

[†]Institute for Physical Chemistry, University of Hamburg, Grindelallee 177, 20146 Hamburg, Germany and [‡]Faculty of Technology and Metallurgy, University of Belgrade, Karnegijeva 4, 11000, Belgrade, Serbia. [§]Both authors contributed equally to this work.

ABSTRACT In this contribution a facile, one-step synthesis of tridentate thiol-functionalized PEO ligands and their ability to stabilize CdSe/CdS/ZnS core—shell—shell nanoparticles in aqueous media are described. The PEO-coated quantum dots show colloidal stability as well as preserved fluorescence even at very low concentrations of a few nM. For improved ligand attachment and enhanced fluorescence properties a method for ligand exchange was developed, which includes formation of a ligand zinc complex before the actual exchange reaction. The stability and fluorescence properties in various aqueous buffers and cell media and at pH values down to pH 3 were investigated. The firm binding of the tridentate ligands to the particle surface makes this ligand—particle system a promising tool for biological applications. In addition, activation of the ligands' terminal hydroxyl group for covalent biofunctionalization by esterification with succinic acid is reported.

KEYWORDS: polyethylene oxide · poly(ethylene glycol) · ligands · water-soluble · CdSe/CdS/ZnS · quantum dots · photoluminescence

Due to their unique optical properties such as broad absorption and narrow emission bands, high photostability, and high quantum yields,[1−3] fluorescent semiconductor nanoparticles (quantum dots, QDs) are used increasingly for biological imaging and labeling.[4−8] In the past decade, significant work was directed toward coupling fluorescent nanoparticles to biomolecules.[9−11] These conjugates found application in cell imaging, FRET assays, drug delivery, and tumor targeting.[6,11−16]

For the transfer of as-synthesized hydrophobic nanoparticles into aqueous media it is necessary to replace the ligands usually used in QD synthesis by appropriate hydrophilic molecules. One of the most promising systems for this purpose are functionalized polyethylene oxides (PEOs), which combine both hydrophilicity and biocompatibility and are considered to be nonimmunogenic, nonantigenic, and nontoxic[17] and provide long blood circulation times.[18,19]

In the past hydrophilic quantum dots were often generated by ligand exchange with thiocarbonic acids such as mercaptopropionic or mercaptoundecanoic acid.[20,21] As it can be assumed that ligands coordinated on particle surfaces are always in equilibrium with free ligands in solution, multidentate anchoring groups should allow for a more stable binding to the particle surface and reduction of dissociation of the particle—ligand system at lower free-ligand concentrations. Several publications mention the use of dihydrolipoic acid (DHLA) or its PEO derivatives as stabilizing ligands for aqueous systems.[22−24] However, particles prepared by this method still have the problem of losing their stability in solutions at pH lower than 5 to 6, when thiols and carboxy groups are protonated and surface charge and ligand affinity are lost.[22,25,26] Nevertheless, for some biological or medical applications it is necessary that quantum dots remain stable in acidic environments such as tumor tissue[27] or endosomes.[28]

In recent years several research groups have shown that thiol-based hydrophilic ligands tend to quench the fluorescence intensity of quantum dots.[29,30] Mattoussi and co-workers have reported on a class of branched, chelating PEO ligands with multiple DHLA moieties that preserved particle fluorescence and colloidal stability down to pH values of 4 and reduced emission at pH values of 1.6.[31] Liu *et al.* have enhanced the fluorescence of water-soluble CdSe/ZnS particles capped with dihydrolipoic acid or cysteine by forming a ligand—Zn complex prior to ligand exchange in a two-phase reaction.[32] They propose a metathesis reaction between the Zn—thiol complex and the surface-bound phosphonic acids of the hydrophobic particles, which leads to a ligand exchange without surface etching by the thiols.

In this paper we present a facile one-step synthesis for a new, tridentate ligand and a

* Address correspondence to weller@chemie.uni-hamburg.de.

Received for review March 21, 2011 and accepted May 27, 2011.

Published online May 27, 2011
10.1021/nn201065y

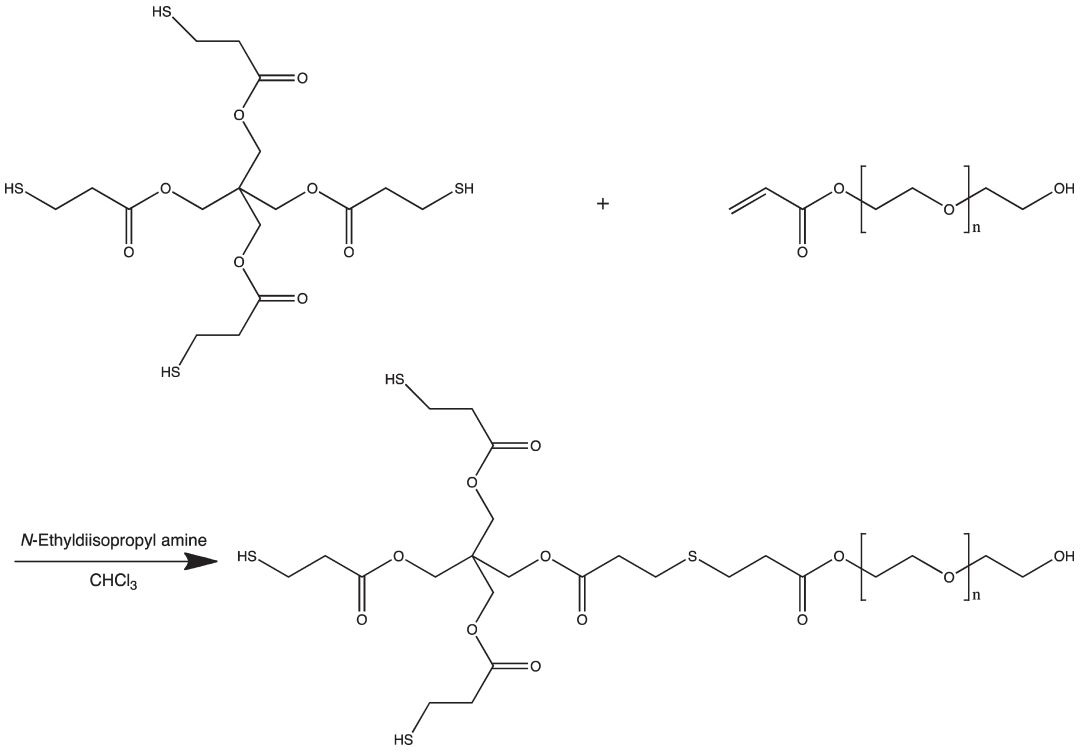

Scheme 1. Synthesis of Tridentate PEO Ligands in a Michael-Type Reaction

ligand exchange method for CdSe/CdS/ZnS particles that is based on a similar precomplexation with Zn^{2+} ions, which is crucial for effective ligand exchange. It enhances the efficiency of ligand exchange and preserves the fluorescence quantum yield to a sufficient degree after transferring the particles into aqueous media. The particles exhibit comparable colloidal stability to the ones capped with branched DHLA-based ligands at low pH.

For most biological applications it is necessary that quantum dots remain stable in different biological buffer systems with various pH values as well as in lowest concentrations. Our ligands provide a system of hydrophilic quantum dots, which show no decrease of fluorescence quantum yield even at high dilution. The prepared particle solutions are stable against dialysis or ultrafiltration, which is required for removing excess ligand after ligand exchange reaction and for concentrating the quantum dot solutions.

RESULTS AND DISCUSSION

Ligand Exchange. Tridentate, water-soluble ligands with an average of three thiol groups were synthesized in a simple one-step reaction using commercially available polyethylene oxide monoacrylate (Scheme 1). The reaction was monitored by ^{1}H NMR, which showed complete conversion of the educts by the disappearance of the acrylate peaks (Figure 1). For the ligand exchange the $PEO(SH)_3$ was precomplexated with Zn^{2+} ions by adding a 0.2 M solution of zinc acetate dihydrate in TOP to a chloroform solution of the ligand and precipitating twice with hexane. The complexation proved to be essential for a reproducible ligand exchange and high quantum yields. Without zinc or by precipitating zinc acetate in TOP together with the particles in chloroform prior to ligand exchange instead of precomplexating the ligands resulted in particles that were only partially soluble in water after several hours in the ultrasonic bath and had significantly reduced quantum yields of ~5%. The effect of zinc was more pronounced with the tridentate ligands than with monodentate $PEO(SH)_1$, leading to the assumption that the chelating effect of $PEO(SH)_3$ increases the affinity to the metal ions. These results confirm the reports by Liu *et al.*[32] that zinc ions play an important role in the ligand exchange of ZnS-coated particles with thiol ligands. Further investigations are necessary to establish the role of zinc in the exchange mechanism.

The ligand was found to degrade slowly over the course of several weeks when stored at −20 °C in the dark under nitrogen atmosphere. Compared to freshly prepared ligands, aged samples required more time of sonication to dissolve in chloroform or water at any step of the ligand exchange procedure. This finding was attributed to oxidation of the thiol groups to disulfides by residual oxygen contained within the material. PEO-coated particles in water did not show a comparable degradation and are stable for several months.

Absorption and emission spectra were measured from the original TOP/TOPO/TDPA-coated quantum dots, from the quantum dots after ligand exchange with

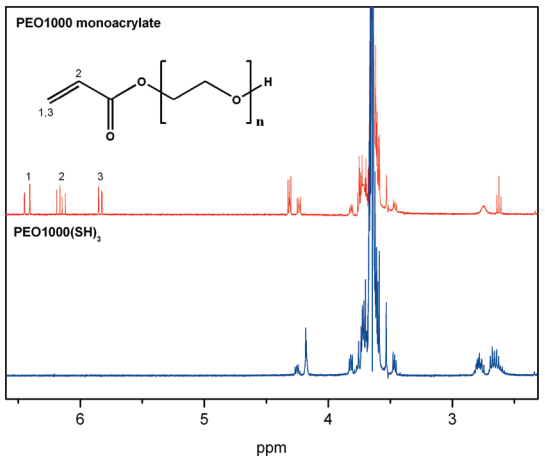

Figure 1. ^{1}H NMR spectra of polyethylene oxide monoacrylate (top) and the ligand PEO1000(SH)$_3$ (bottom). The disappearance of the acrylate peaks at 5.8−6.4 ppm indicates complete conversion of the polymer.

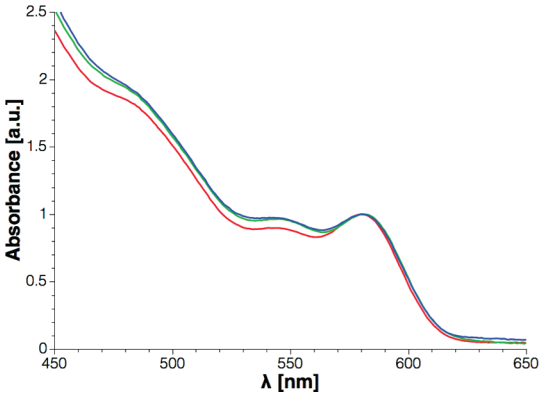

Figure 2. Normalized UV−vis absorption spectra of CdSe/CdS/ZnS nanoparticles before ligand exchange in toluene (red) and after ligand exchange in chloroform (green) and water (blue).

PEO(SH)$_3$ with various chain lengths, and from the PEO-coated quantum dots after transfer into water. For all ligands investigated there was no significant change in the absorption spectra after ligand exchange. Normalized emission spectra showed only small changes in emission wavelength. Transfer into chloroform from toluene during the ligand exchange procedure caused a slight blue shift (1−4 nm), whereas a small red shift (4−10 nm) occurred after transfer of the particles into water. Similar results were previously reported by Bawendi and co-workers and can be explained as solvatochroistic effects.[35,36] Figures 2 and 3 show spectra of particles coated with PEO1000(SH)$_3$.

Quantum yields (QYs) were measured for quantum dots before and after ligand exchange and after transfer into water. As described previously, the ligand exchange caused a decrease in luminescence QY of about 2−3%, and an additional decrease of photoluminescence (PL) intensity was observed after transfer into water to about half of the QY of the original TOP/TOPO-coated particles.

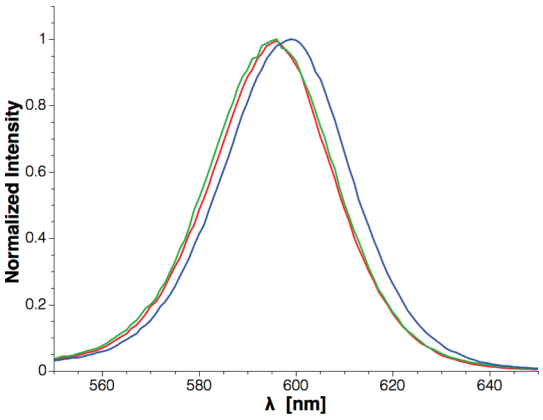

Figure 3. Emission spectra of CdSe/CdS/ZnS nanoparticles before ligand exchange in toluene (red) and after ligand exchange in chloroform (green) and water (blue).

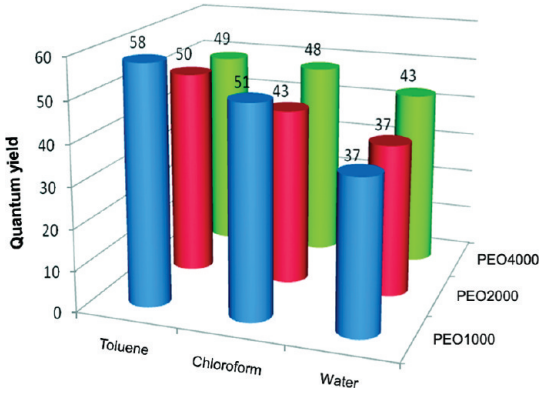

Figure 4. Fluorescence quantum yields of the particles in toluene before ligand exchange, in chloroform after ligand exchange, and after transfer into water. Different PEO chain lengths were employed: PEO1000(SH)$_3$ (blue), PEO2000-(SH)$_3$ (red), and PEO4000(SH)$_3$ (green).

This decrease in PL QY was independent of the PEO chain lengths corresponding to molecular weights of 1000 to 4000 g/mol (Figure 4). However, for chain lengths below a molecular weight of 1000 g/mol no solubility in water was obtained with tridentate ligands. Therefore these short ligands were not used in further experiments reported here. We note that for longer ligands above 1000 g/mol a quantum dot to ligand ratio below 4500 led to agglomerated particles and significantly lower quantum yields. This was attributed to incomplete surface coverage by the ligands, which causes the agglomeration of uncovered surfaces due to hydrophobic interactions. The lower quantum yield of these samples can be explained by self-quenching of the particle aggregates.[37]

TEM pictures in Figure 5 show a typical sample of PEO-modified quantum dots in chloroform and water. The pictures show that the sample consisted predominantly of individual particles, and the narrow size distribution of 6.2 ± 0.7 nm was preserved.

To determine the hydrodynamic diameter of the PEO-coated particles, dynamic light scattering (DLS)

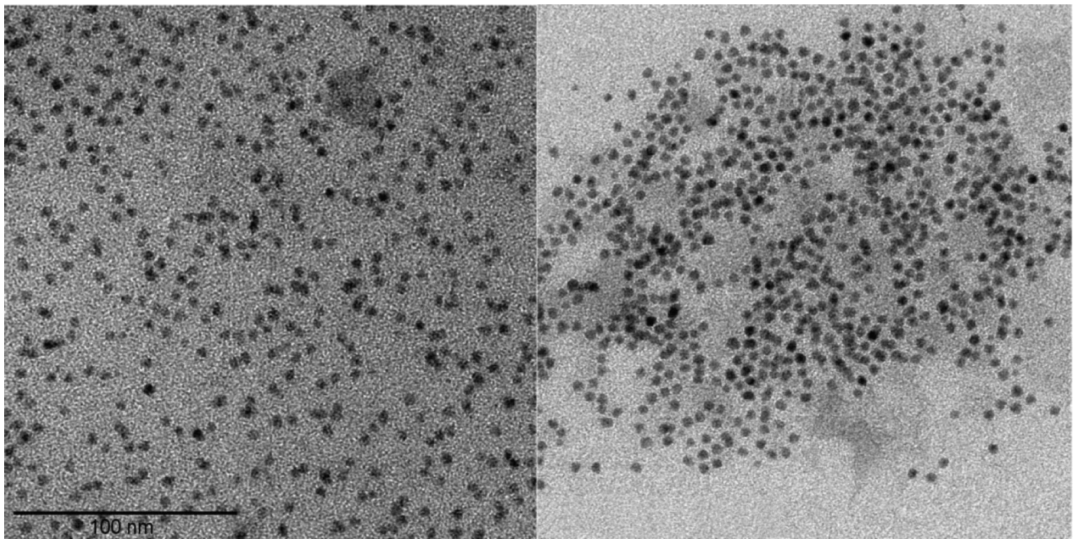

Figure 5. TEM pictures of PEO1000(SH)$_3$-coated quantum dots deposited from chloroform (left) and water (right). The apparent aggregation of particles in water is due to different wetting behaviors of the solvents on the TEM grid.

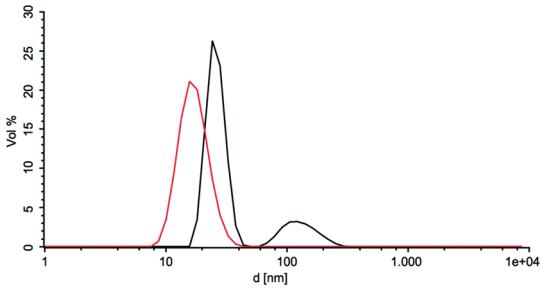

Figure 6. DLS distribution by volume of CdSe/CdS/ZnS quantum dots stabilized by PEO1000(SH)$_3$ in water. Black curve: Distribution of freshly prepared sample; red curve: distribution of sample purified by size exclusion HPLC.

measurements of the aqueous solutions were performed. The hydrodynamic diameters of single particles were ~25 nm, which comprises the size of the inorganic core, length of the PEO chains, and solvatization shell. No clear influence of the ligand chain length on the hydrodynamic diameters could be observed. This finding indicates a decreasing number density of attached ligands with increasing PEO chain length (see discussion of zeta potentials below). The results showed that there was always a small amount of agglomerates of a size about 100 nm next to the single particles (Figure 6, black curve). Since the radius of the agglomerates contributes to the peak intensity in a volume-weighted distribution as a power of 3, the total number of agglomerates is rather low. We assume that the reason for the formation of these agglomerates is due to interaction between the PEO chains of several particles, which entangle during the precipitation steps.

These agglomerates had no negative effects on the following results, but could cause problems in further applications. It was possible to separate those agglomerates by size exclusion HPLC. The fractions containing the single particles were concentrated by ultrafiltration (Vivaspin) and examined by DLS (Figure 6, red curve). The samples were monitored for 2 days, and formation of new agglomerates was not observed. Fluorescence properties were not changed during these procedures.

Ligand exchange and transfer into water with PEO-(SH)$_3$ could also be successfully performed with PbS, PbS/ZnS, InP/ZnS, and Au nanoparticles (see Supporting Information).

Dependency of the Stability on Concentration and pH. In order to assess the ligand–QD stability, a dilution series of hydrophilic particles capped with either monodentate or tridentate PEO2000-thiol ligands was prepared from a stock solution, and the change in fluorescence intensity was measured over a period of 128 min.

At pH 7 in bidistilled H_2O the emission of particles capped with the tridentate ligand was stable during the measurement for all concentrations down to dilutions below 5 nM (Figure 7B). The monodentate ligand showed a comparable stability with a 10% drop of initial fluorescence intensity after 1 h for the most diluted sample at 5 nM (Figure 7A). Neither system showed a significant decrease in quantum yield for the freshly diluted samples. The initial values for the quantum yields were 20% in water using the monodentate ligand and 30–40% with the tridentate ligand.

When the ligand–QD system was destabilized by adjusting the pH to 5 with a 0.1 M acetate buffer, both particle systems showed decreased fluorescence with increasing dilution below a certain particle concentration. For the particles capped with PEO2000(SH)$_1$ a 10% lower emission intensity was measured below a concentration of 180 nM after 2 h, and at a concentration of 5 nM the emission had dropped to 50% after 2 h (Figure 8A). PEO2000(SH)$_3$-capped particles showed a significant decrease in fluorescence intensity (10%) only at 3.6 times higher dilutions at 50 nM (Figure 8B). Below

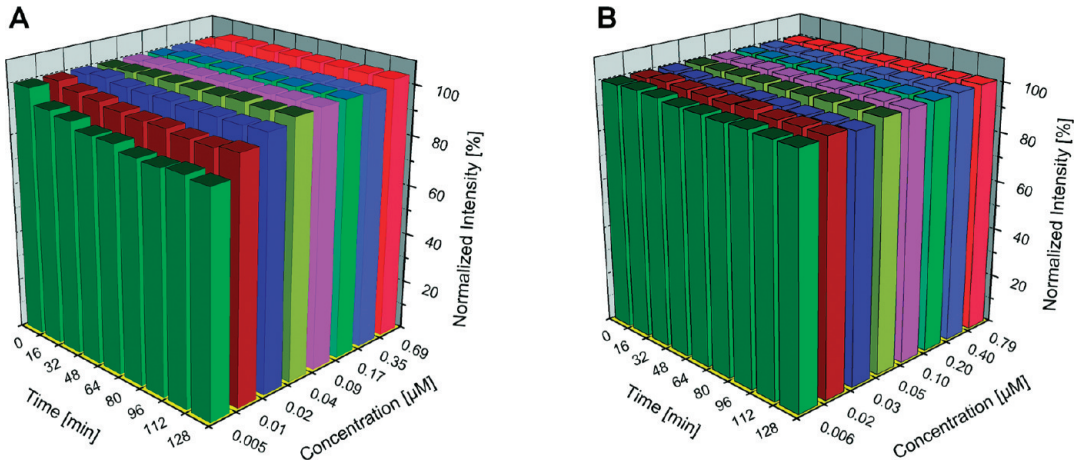

Figure 7. Normalized fluorescence intensities of CdSe/CdS/ZnS quantum dots coated with PEO2000(SH) (A) and PEO2000(SH)$_3$ (B) at pH 7 as a function of particle concentration and time. The particles capped with tridentate ligands are stable against dilution, while monodentate-capped particles show a slight decrease of fluorescence intensity at concentrations below 20 nM.

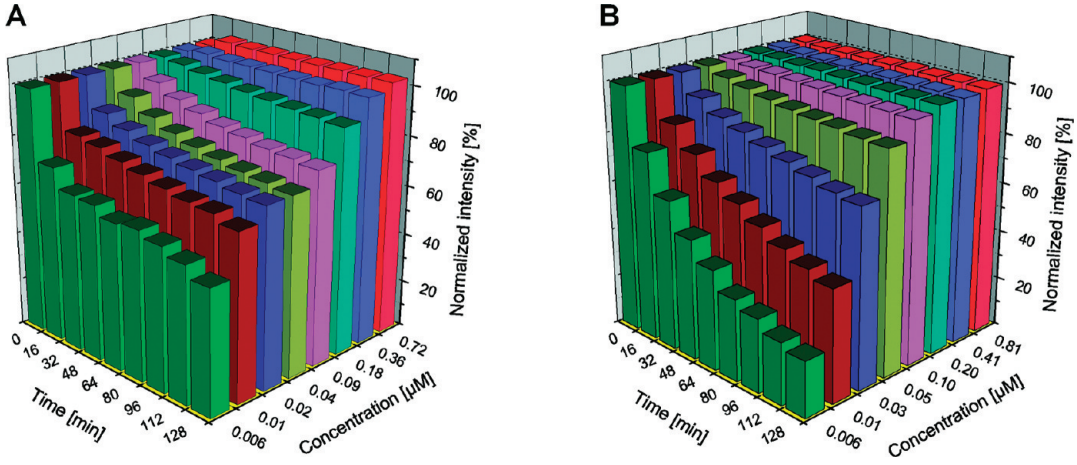

Figure 8. Normalized fluorescence intensities of CdSe/CdS/ZnS quantum dots coated with PEO2000(SH) (A) and PEO2000-(SH)$_3$ (B) at pH 5 as a function of particle concentration and time. Particles capped with the tridentate ligand can be diluted to a 4 times lower concentration before a significant change in fluorescence intensity occurs. The detachment of the tridentate ligand follows a monoexponential decay, while the monodentate ligand shows two distinct rate constants.

that concentration the intensity dropped more quickly, and 22% of the initial intensity remained after 2 h for a concentration of 6 nM.

It is remarkable that the decay of fluorescence intensity followed monoexponential desorption kinetics in the case of the more complex chelating ligand, while the data for the monofunctional ligand could be fitted with a biexponential decay function with a fast component of 8 min^{-1} and a very slow component. Since the decline of the fluorescence intensity can be directly correlated to the ligand detachment from the particle surface,[38−41] this behavior indicates two distinct ways for the monodentate ligand to bind to and be detached from the particle surface. The finding can be explained by assuming that only part of the ligands is bound to a zinc ion, thus creating two binding species. This is supported by the fact that when no zinc is used for the ligand exchange, the particles' fluorescence intensity is also reduced monoexponentially, although with a much lower initial quantum yield below 10%.

Throughout the tested pH range from 8 to 3 the tridentate ligands stabilized the particles and showed little or no change in fluorescence quantum yield after equilibration at relatively high particle concentrations (0.3 μM), while monodentate ligand-capped particles show poor stability below a pH of 5 (Figure 9, top). Both ligands can be destabilized at lower concentrations (0.05 μM), but the tridentate ligand maintains luminescence, whereas the particles capped with monodentate ligands start to aggregate below a pH of 5 and have no detectable emission below a pH of 4. These findings are comparable to tetradentate DHLA-based ligands described by Mattoussi and co-workers.[31]

Samples from pH 3 to pH 5 were prepared in acetate buffer (0.01 M); samples with pH 6 and 7, in phosphate buffer (0.01 M).

Buffer Tests. For biological applications the stability of hydrophilic particles in various aqueous solutions such as buffers and cell media is very important.

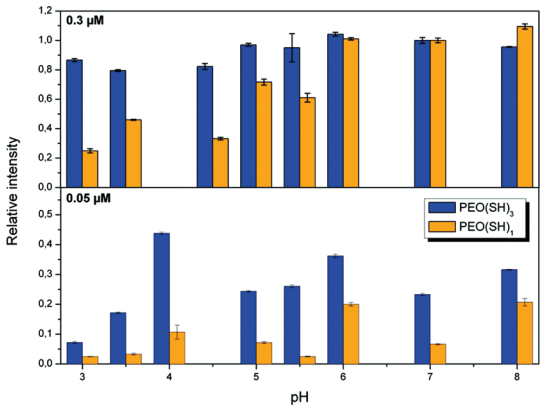

Figure 9. Fluorescence intensity of particles capped with mono- and tridentate PEO ligands at different pH values in equilibrium. At high concentrations (0.3 μM, top) the tridentate ligands are stable throughout the whole range of displayed pH values, while particles with monodentate ligands show reduced luminescence below a pH value of 6. At low concentrations (0.05 μM, bottom) and below pH 4 the sample containing monodentate ligands has no luminescence above the detection limit. The fluorescence intensity has been normalized to the value for pH 7 at 0.3 μM. The data points at pH 4 (0.3 μM) and pH 4.5 (0.05 μM) were excluded, because the particles precipitated before the measurement.

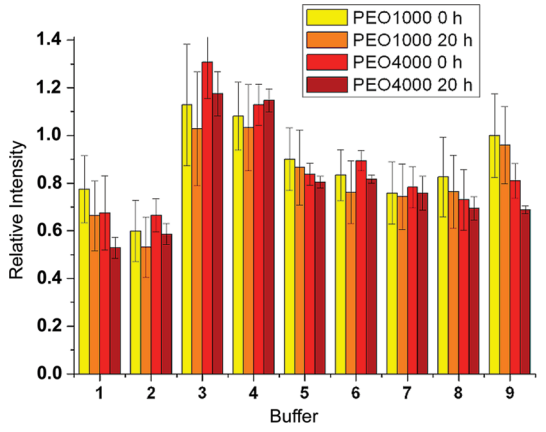

Figure 10. Fluorescence of CdSe/CdS/ZnS quantum dots coated with different chain length PEO(SH)$_3$ in various buffer media at a concentration of 0.2 μM: 1. DMEM; 2. HEPES/DMEM; 3. TRIS-HCl (pH 8); 4: EGTA (pH 8.5, 0.1 M); 5: EDTA (pH 8, 1 mM); 6: NaCl (1 M); 7: MOPS/SDS; 8: DPBS; 9: H_2O. (The data were normalized to the value of PEO1000/H_2O at 0 h.)

Figure 10 shows the PL intensity in a selection of typical buffer solutions, in the presence of complexing agents such as EDTA as well as in Dulbecco's modified Eagle medium (DMEM).

Nearly all samples with tridentate ligands showed well-preserved PL intensity independent of pH, composition, or ionic strength over a period of 20 h. There was no remarkable effect of the PEO chain length and only a small decrease in PL intensity after the investigated period. Cell media show a small decrease in PL emission, which is assumed to be due to phenol red in the medium, which has a strong influence on the absorption behavior of the sample, causing inner filter effects.

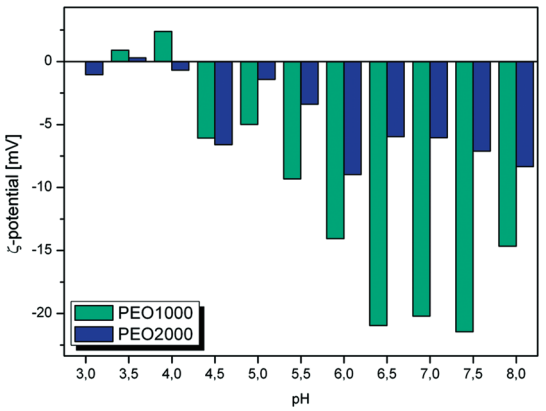

Figure 11. Zeta potential of carboxy-functionalized particles correlated to pH. Blue: quantum dots coated with PEO1000(SH)$_3$-succinic ester; cyan: quantum dots coated with PEO2000(SH)$_3$-succinic ester.

Activation of the Terminal Hydroxyl Group. To enable functionalization of PEO-coated particles by EDC/Sulfo-NHS coupling, the used PEO monoacrylates were activated by reaction with succinic anhydride. ^{1}H NMR spectroscopy showed that the acrylic terminus stayed intact and characteristic signals could be assigned to the protons belonging to the succinic ester (see Supporting Information).

After ligand exchange with the carboxy-functionalized ligands, the zeta potential of the particles was measured at different pH values. Zeta potentials smaller than $\pm$2.5 mV were measured for pH values below 4, where the particles are uncharged. At higher pH values the surface charge increases due to deprotonation of the terminal carboxylic groups, which are completely deprotonated above pH 6.5 (Figure 11). At high pH the difference in zeta potentials between PEO1000(SH)$_3$ ($-$20 mV) and PEO2000(SH)$_3$ ($-$5 mV) is attributed to a different degree of surface coverage, with shorter ligands having a higher number density on the particle surface than longer ones. This explains the DLS results, indicating independence of the hydrodynamic diameter on the chain length of the ligands. It implies that the footprint of the ligands increases with increasing molecular mass due to coiling and backfolding of the PEO chain.

Hydroxy-functionalized particles showed no pH dependence of the zeta potential, which had a value of $\pm$2 mV (data not shown).

CONCLUSIONS

A new thiol ligand with multiple anchoring groups was presented, which is both easily synthesized and enables a simple and reproducible ligand exchange for a broad range of nanoparticles. It was found that complexing the thiols with zinc ions prior to the ligand exchange greatly enhances the fluorescence quantum yield of CdSe/CdS/ZnS particles in aqueous media. Due to its tridentate character, the ligand binds more strongly to

the particle surface than a monodentate PEO thiol and the surface equilibrium is shifted toward the ligand–particle complex. Therefore the here-described ligand system promotes high stability and conservation of PL intensity in very low concentrations as well as in different biologically relevant buffers and cell media and in a wide pH range. By esterification with succinic acid, functionalizable quantum dots were obtained, which could be employed for biofunctionalization in a wide range of biological or medical applications. Due to the high binding affinity of the thiol groups to metal ions and atoms, the ligands are suitable for stabilization of a wide range of nanoparticles, for example gold or III–V semiconductor particles.

EXPERIMENTAL SECTION

Materials. Milli-Q water (Millipore) was used as bidistilled water. All solvents were of analytical grade and purchased from Merck or Sigma-Aldrich. PEO monomethyl ether was purchased from Merck, PEO monoacrylate was purchased from Monomer-Polymer & Dajac Labs, Inc., and pentaerythritol tetrakis(3-mercaptopropionate) and 11-mercaptoundecanoic acid (MUA) were purchased from Aldrich and used without purification. *N*-Ethyldiisopropylamine sealed under inert gas in a crown cap bottle was purchased from Aldrich. Zinc acetate dihydrate and trioctylphosphine (TOP) were purchased from Fluka. Rhodamine 6G (laser grade) was purchased from Lambda Physik. Dulbecco's modified Eagle medium (DMEM) (1×) liquid (low glucose) containing 1000 mg/L D-glucose and L-glutamine and 110 mg/L sodium pyruvate by Invitrogen was used as the cell medium in the stability test. All buffers were made from chemicals purchased from Merck, except tris(hydroxymethyl)-aminomethane (TRIS), which was purchased from Fluka.

The synthesis of CdSe/CdS/ZnS core–shell–shell particles followed previously published protocols.[3,33] The particle size was determined by TEM analysis. The concentrations of colloidal solutions were estimated from the first absorption maximum using an empirical formula developed by Peng and co-workers for CdSe cores.[34] The calculated concentration is expected to be approximately 50% too low due to the systematical error of applying the formula on core–shell–shell particles. This is acceptable for a rough estimation of the particle concentration (see Supporting Information).

Characterization. UV–vis absorption spectra were measured at room temperature with a Cary 50 UV–vis spectrometer (Varian). Photoluminescence spectra and high-throughput screening of well plates were measured at room temperature with a Cary Eclipse Spectrometer (Varian).

Dilution experiments and kinetic measurements were performed using a Fluorolog-3 spectrometer (Horiba Jobin Yvon). TEM images were measured with a Jeol JEM 1011 EM electron microscope operating at 100 kV. Samples for TEM investigations were prepared by dropping dilute solutions of properly washed nanocrystals in chloroform or water onto 400-mesh carbon-coated copper grids, with subsequent removal of the solvent by filter paper. DLS and zeta potential measurements were performed using a Zeta Sizer Nano-ZS (Malvern Instruments). Dialysis of aqueous particle solutions was performed using a Spectrapor Float-a-Lyzer (Roth). For concentration of aqueous particle solutions Vivaspin 500 centrifugal units with a MWCO of 10 kD were employed.

HPLC measurements and particle purifications were performed with an Akta Purifier 10 (GE Healthcare) equipped with a Superdex 200 10-30 column.

Monodentate PEO(SH)$_1$ Ligand Synthesis. Six grams (~5 mmol) of PEO monomethyl ether (M = 2000 g/mol) and 3.28 g (15 mmol) of MUA were added to a 50 mL flask and stirred at 160 °C for 72 h under inert gas atmosphere. After the reaction was complete the reaction mixture was cooled to 60 °C and dissolved in 3.5 mL of chloroform. The solution was precipitated in 50 mL of cold diethyl ether, and the precipitate was collected by vacuum filtration and washed repeatedly with cold diethyl ether. In order to remove the excess of MUA, the precipitate was dissolved in water, the undissolved MUA was filtered off, and the solution was lyophilized. The turnover was determined to be >95% based on NMR data.

Tridentate PEO(SH)$_3$ Ligand Synthesis. Synthesis of tridentate, thiol-functionalized PEO ligands followed a Michael-type reaction, where PEO-monoacrylates of different chain lengths (M = 500, 1000, 2000, or 4000 g/mol) were coupled to pentaerythritol tetrakis(3-mercaptopropionate) (Scheme 1).

In a typical synthesis 2 equiv (4 mmol) of PEO monoacrylate was dissolved in 25 mL of chloroform, and 1 equiv (2 mmol, 764 μL) of pentaerythritol tetrakis(3-mercaptopropionate) and 4 equiv (8 mmol, 1.4 mL) of *N*-ethyldiisopropyl amine were added. The solution was stirred at 50 °C for 72 h. After cooling to room temperature, the ligand was precipitated twice by adding the solution dropwise to diethyl ether at −20 °C. The white precipitate was collected by vacuum filtration, dried under vacuum, and stored in the dark at −20 °C. Formation of the ligand can be monitored by ^{1}H NMR spectroscopy, where the disappearance of the characteristic acrylate peaks indicates complete conversion of the educts (Figure 1).

Synthesis of Carboxyl-Terminated PEO. To obtain ligands with a carboxy terminus, 1 equiv (4 mmol) of PEO monoacrylate was dissolved in anhydrous chloroform. Then 0.2 equiv (0.8 mmol, 0.088 g) of 4-dimethylaminopyridine and 5 equiv (20 mmol, 2 g) of succinic anhydride were added, and the solution was stirred at room temperature overnight. The reaction mixture was extracted three times with saturated NaCl solution and dried over anhydrous sodium sulfate. The product was then precipitated in diethyl ether at −20 °C and used for the ligand synthesis as described above. The success of the reaction was verified by ^{1}H NMR. The reaction had a yield of 64%.

Ligand Exchange. In order to prepare hydrophilic quantum dots, tridentate ligands were dissolved in chloroform, and 1 equiv of zinc acetate dihydrate in TOP (0.2 M) was added. The immediately formed ligand–zinc complex was precipitated with hexane and redissolved in chloroform two times to remove excessive TOP. QDs with a diameter of about 5 nm were added in a ligand/quantum dot ratio of 4500:1, and the solution was stirred for 4 h. Afterward the particles were precipitated two times by adding hexane, and the precipitate was dried and dissolved in bidistilled water by sonicating. Excess ligand was removed by dialysis in Float-a-Lyzers with a MWCO of 5000 g/mol for ligands with PEO chains of M = 400, 1000 (PEO1000(SH)$_3$), and 2000 g/mol (PEO2000(SH)$_3$) and a MWCO of 8000 for ligands with PEO chains of M = 4000 g/mol (PEO4000(SH)$_3$). The particle solutions were then purified by preparative HPLC, concentrated by ultrafiltration, and stored in the dark until further use. Ligand exchange with the monodentate thiol-PEO ligand was performed analogously.

UV–Vis and PL Measurements. The PL emission spectra of colloid nanoparticle solutions were recorded from samples having optical densities below 0.1 at the excitation wavelength, in order to avoid different attenuation of exciting light beam and reabsorption of emitted light.

The values for PL quantum yields at room temperature were determined by comparing the integrated PL intensity of the nanocrystal sample with that of a solution of Rhodamin 6G in absolute ethanol. The wavelength of the intersection of the absorption spectra was used as the excitation wavelength in the PL experiments in order to have the same absorption for both samples. The quantum yield was calculated relative to the

literature value of 0.95 for Rhodamin 6G at room temperature. There were no further corrections performed. The errors resulting from different refraction indices of the solvents are smaller than 5%, and the total error of this method for quantum yield calculation is about 10%.[3]

Buffer Tests and Measurement of PL Intensity Correlated to Particle Concentration. Particles coated by PEO ligands with various chain lengths were dissolved in the following aqueous media: Dulbecco's modified Eagle medium (DMEM), *N*-2-hydroxyethylpiperazine-*N*′-2-ethanesulfonic acid (HEPES)/DMEM, TRIS-HCl (pH 8), ethylene glycol tetraacetic acid (EGTA, pH 8.5, 0.1 M), ethylenediaminetetraacetic acid (EDTA, pH 8, 1 mM); NaCl (1 M); 1−4-morpholinepropanesulfonate sodium dodecyl sulfate (MOPS SDS); Dulbecco's phosphate-buffered saline (D-PBS) with $CaCl_2$ and $MgCl_2$ (DPBS), and bidistilled H_2O.

A stock solution of core−shell−shell particles in water (particle concentration 1 μmol/L) was prepared and then added to the various buffers and media to a final concentration of 0.1 μmol/L. The solutions were measured in 96-well plates using a Varian Cary Eclipse plate reader.

The measurements were performed immediately after preparation of the samples and again after 20 h. The well plate was stored in the dark at 4 °C and reequilibrated to room temperature before the measurement. For the buffer test, PL emission curves were integrated and compared to an equivalent sample of particles in pure water.

Acknowledgment. The authors would like to thank Dr. V. Sinnwell from the Institute of Organic Chemistry for NMR measurements, Sylvia Bartholdi-Nawrath for TEM measurements, and Katja Werner from the Center of Applied Nanotechnology (CAN) for assistance in HPLC measurements. Funding was provided by the priority programme DFG-SPP 1313 of the Deutsche Forschungsgemeinschaft (WE2059/8-1).

Supporting Information Available: NMR spectrum for PEO1000$(SH)_3$ succinic ester. Results for ligand exchange with Au and InP/ZnS core/shell nanoparticles. Discussion on the systematical error for the calculation of particle concentrations. This material is available free of charge *via* the Internet at http://pubs.acs.org.

REFERENCES AND NOTES

1. Grecco, H. E.; Lidke, K. A.; Heintzmann, R.; Lidke, D. S.; Spagnuolo, C.; Martinez, O. E.; Jares-Erijman, E. A.; Jovin, T. M. Ensemble and Single Particle Photophysical Properties (Two-Photon Excitation, Anisotropy, FRET, Lifetime, Spectral Conversion) of Commercial Quantum Dots in Solution and in Live Cells. *Microsc. Res. Tech.* **2004**, *65*, 169–79.
2. Eychmüller, A. Structure and Photophysics of Semiconductor Nanocrystals. *J. Phys. Chem. B* **2000**, *104*, 6514–6528.
3. Mekis, I.; Talapin, D. V.; Kornowski, A.; Haase, M.; Weller, H. One-Pot Synthesis of Highly Luminescent CdSe/CdS Core-Shell Nanocrystals via Organometallic and "Greener" Chemical Approaches. *J. Phys. Chem. B* **2003**, *107*, 7454–7462.
4. Bagalkot, V.; Zhang, L.; Levy-Nissenbaum, E.; Jon, S.; Kantoff, P. W.; Langer, R.; Farokhzad, O. C. Quantum Dot-Aptamer Conjugates for Synchronous Cancer Imaging, Therapy, and Sensing of Drug Delivery Based on Bi-Fluorescence Resonance Energy Transfer. *Nano Lett.* **2007**, *7*, 3065–3070.
5. Baron, R.; Willner, B.; Willner, I. Biomolecule-Nanoparticle Hybrids as Functional Units for Nanobiotechnology. *Chem. Commun.* **2007**, *4*, 323–32.
6. Michalet, X.; Pinaud, F. F.; Bentolila, L. A.; Tsay, J. M.; Doose, S.; Li, J. J.; Sundaresan, G.; Wu, A. M.; Gambhir, S. S.; Weiss, S. Quantum Dots for Live Cells, in Vivo Imaging, and Diagnostics. *Science* **2005**, *307*, 538–544.
7. Medintz, I. L.; Uyeda, H. T.; Goldman, E. R.; Mattoussi, H. Quantum Dot Bioconjugates for Imaging, Labelling and Sensing. *Nat. Mater.* **2005**, *4*, 435–446.
8. Gopalakrishnan, G.; Danelon, C.; Izewska, P.; Prummer, M.; Bolinger, P.-Y.; Geissbuhler, I.; Demurtas, D.; Dubochet, J.; Vogel, H. Multifunctional Lipid/Quantum Dot Hybrid Nanocontainers for Controlled Targeting of Live Cells. *Angew. Chem., Int. Ed.* **2006**, *45*, 5478–5483.
9. Bruchez, M., Jr.; Moronne, M.; Gin, P.; Weiss, S.; Alivisatos, A. P. Semiconductor Nanocrystals as Fluorescent Biological Labels. *Science* **1998**, *281*, 2013–2016.
10. Young, S. H.; Rozengurt, E. Qdot Nanocrystal Conjugates Conjugated to Bombesin or ANG II Label the Cognate G Protein-Coupled Receptor in Living Cells. *Am. J. Physiol.* **2006**, *290*, C728–C732.
11. Goldman, E. R.; Balighian, E. D.; Mattoussi, H.; Kuno, M. K.; Mauro, J. M.; Tran, P. T.; Anderson, G. P. Avidin: A Natural Bridge for Quantum Dot-Antibody Conjugates. *J. Am. Chem. Soc.* **2002**, *124*, 6378–6382.
12. Chen, A. A.; Derfus, A. M.; Khetani, S. R.; Bhatia, S. N. Quantum Dots to Monitor RNAi Delivery and Improve Gene Silencing. *Nucleic Acids Res.* **2005**, *33*, 190.
13. Courty, S.; Luccardini, C.; Bellaiche, Y.; Cappello, G.; Dahan, M. Tracking Individual Kinesin Motors in Living Cells Using Single Quantum-Dot Imaging. *Nano Lett.* **2006**, *6*, 1491–1495.
14. Lidke, D. S.; Nagy, P.; Heintzmann, R.; Arndt-Jovin, D. J.; Post, J. N.; Grecco, H. E.; Jares-Erijman, E. A.; Jovin, T. M. Quantum Dot Ligands Provide New Insights into erbB/HER Receptor-Mediated Signal Transduction. *Nat. Biotechnol.* **2004**, *22*, 198–203.
15. Alivisatos, A. P.; Gu, W.; Larabell, C. Quantum Dots as Cellular Probes. *Annu. Rev. Biomed. Eng.* **2005**, *7*, 55–76.
16. Medintz, I. L.; Clapp, A. R.; Mattoussi, H.; Goldman, E. R.; Fisher, B.; Mauro, J. M. Self-Assembled Nanoscale Biosensors Based on Quantum Dot FRET Donors. *Nat. Mater.* **2003**, *2*, 630–638.
17. Goelander, C. G.; Herron, J. N.; Lim, K.; Claesson, P.; Stenius, P.; Andrade, J. D. Properties of Immobilized PEG Films and the Interaction with Proteins. Experiments and Modeling. *Poly(Ethylene Glycol) Chem.* **1992**, 221–245.
18. Choi, H. S.; Ipe, B. I.; Misra, P.; Lee, J. H.; Bawendi, M. G.; Frangioni, J. V. Tissue- and Organ-Selective Biodistribution of NIR Fluorescent Quantum Dots. *Nano Lett.* **2009**, *9*, 2354–2359.
19. Prencipe, G.; Tabakman, S. M.; Welsher, K.; Liu, Z.; Goodwin, A. P.; Zhang, L.; Henry, J.; Dai, H. PEG Branched Polymer for Functionalization of Nanomaterials with Ultralong Blood Circulation. *J. Am. Chem. Soc.* **2009**, *131*, 4783–4787.
20. Chan, W. C.; Nie, S. Quantum Dot Bioconjugates for Ultrasensitive Nonisotopic Detection. *Science* **1998**, *281*, 2016–2018.
21. Reiss, P.; Bleuse, J.; Pron, A. Highly Luminescent CdSe/ZnSe Core/Shell Nanocrystals of Low Size Dispersion. *Nano Lett.* **2002**, *2*, 781–784.
22. Mattoussi, H.; Mauro, J. M.; Goldman, E. R.; Anderson, G. P.; Sundar, V. C.; Mikulec, F. V.; Bawendi, M. G. Self-Assembly of CdSe-ZnS Quantum Dot Bioconjugates Using an Engineered Recombinant Protein. *J. Am. Chem. Soc.* **2000**, *122*, 12142–12150.
23. Uyeda, H. T.; Medintz, I. L.; Jaiswal, J. K.; Simon, S. M.; Mattoussi, H. Synthesis of Compact Multidentate Ligands to Prepare Stable Hydrophilic Quantum Dot Fluorophores. *J. Am. Chem. Soc.* **2005**, *127*, 3870–3878.
24. Liu, W.; Choi, H. S.; Zimmer, J. P.; Tanaka, E.; Frangioni, J. V.; Bawendi, M. Compact Cysteine-Coated CdSe(ZnCdS) Quantum Dots for in Vivo Applications. *J. Am. Chem. Soc.* **2007**, *129*, 14530–14531.
25. Algar, W. R.; Krull, U. J. Luminescence and Stability of Aqueous Thioalkyl Acid Capped CdSe/ZnS Quantum Dots Correlated to Ligand Ionization. *ChemPhysChem* **2007**, *8*, 561–568.
26. Aldana, J.; Lavelle, N.; Wang, Y.; Peng, X. Size-Dependent Dissociation pH of Thiolate Ligands from Cadmium Chalcogenide Nanocrystals. *J. Am. Chem. Soc.* **2005**, *127*, 2496–2504.
27. Robey, I. F.; Baggett, B. K.; Kirkpatrick, N. D.; Roe, D. J.; Dosescu, J.; Sloane, B. F.; Hashim, A. I.; Morse, D. L.; Raghunand, N.; Gatenby, R. A.; *et al.* Bicarbonate Increases Tumor pH and Inhibits Spontaneous Metastases. *Cancer Res.* **2009**, *69*, 2260–2268.

28. Blum, J. S.; Fiani, M. L.; Stahl, P. D. Proteolytic Cleavage of Ricin A Chain in Endosomal Vesicles. Evidence for the Action of Endosomal Proteases at Both Neutral and Acidic pH. *J. Biol. Chem.* **1991**, *266*, 22091–22095.
29. Xie, R.; Kolb, U.; Li, J.; Basche, T.; Mews, A. Synthesis and Characterization of Highly Luminescent CdSe-Core CdS/$Zn_{0.5}Cd_{0.5}S$/ZnS Multishell Nanocrystals. *J. Am. Chem. Soc.* **2005**, *127*, 7480–7488.
30. Breus, V. V.; Heyes, C. D.; Nienhaus, G. U. Quenching of CdSe-ZnS Core-Shell Quantum Dot Luminescence by Water-Soluble Thiolated Ligands. *J. Phys. Chem. C* **2007**, *111*, 18589–18594.
31. Stewart, M. H.; Susumu, K.; Mei, B. C.; Medintz, I. L.; Delehanty, J. B.; Blanco-Canosa, J. B.; Dawson, P. E.; Mattoussi, H. Multidentate Poly(ethylene glycol) Ligands Provide Colloidal Stability to Semiconductor and Metallic Nanocrystals in Extreme Conditions. *J. Am. Chem. Soc.* **2010**, *132*, 9804–9813.
32. Liu, D.; Snee, P. T. Water-Soluble Semiconductor Nanocrystals Cap Exchanged with Metalated Ligands. *ACS Nano* **2011**, *5*, 546–550.
33. Talapin, D. V.; Rogach, A. L.; Kornowski, A.; Haase, M.; Weller, H. Highly Luminescent Monodisperse CdSe and CdSe/ZnS Nanocrystals Synthesized in a Hexadecylamine-Trioctylphosphine Oxide-Trioctylphosphine Mixture. *Nano Lett.* **2001**, *1*, 207–211.
34. Yu, W. W.; Qu, L.; Guo, W.; Peng, X. Experimental Determination of the Extinction Coefficient of CdTe, CdSe, and CdS Nanocrystals. *Chem. Mater.* **2003**, *15*, 2854–2860.
35. Boulmedais, F.; Bauchat, P.; Brienne, M. J.; Arnal, I.; Artzner, F.; Gacoin, T.; Dahan, M.; Marchi-Artzner, V. Water-Soluble Pegylated Quantum Dots: From a Composite Hexagonal Phase to Isolated Micelles. *Langmuir* **2006**, *22*, 9797–9803.
36. Leatherdale, C. A.; Bawendi, M. G. Observation of Solvatochromism in CdSe Colloidal Quantum Dots. *Phys. Rev. B* **2001**, *63*, 165315/1–165315/6.
37. Grabolle, M.; Spieles, M.; Lesnyak, V.; Gaponik, N.; Eychmüller, A.; Resch-Genger, U. Determination of the Fluorescence Quantum Yield of Quantum Dots: Suitable Procedures and Achievable Uncertainties. *Anal. Chem.* **2009**, *81*, 6285–6294.
38. Kalyuzhny, G.; Murray, R. W. Ligand Effects on Optical Properties of CdSe Nanocrystals. *J. Phys. Chem. B* **2005**, *109*, 7012–7021.
39. Sharma, S. N.; Pillai, Z. S.; Kamat, P. V. Photoinduced Charge Transfer between CdSe Quantum Dots and p-Phenylenediamine. *J. Phys. Chem. B* **2003**, *107*, 10088–10093.
40. Leung, K.; Whaley, K. B. Surface Relaxation in CdSe Nanocrystals. *J. Chem. Phys.* **1999**, *110*, 11012.
41. Morris-Cohen, A. J.; Donakowski, M. D.; Knowles, K. E.; Weiss, E. A. The Effect of a Common Purification Procedure on the Chemical Composition of the Surfaces of CdSe Quantum Dots Synthesized with Trioctylphosphine Oxide. *J. Phys. Chem. C* **2010**, *114*, 897–906.